Molecular structure-dependent deformations in boron nitride nanostructures subject to an electrical field

2013 J. Phys. D: Appl. Phys. 46 235303

(http://iopscience.iop.org/0022-3727/46/23/235303)

IOP PUBLISHING JOURNAL OF PHYSICS D: APPLIED PHYSICS

J. Phys. D: Appl. Phys. **46** (2013) 235303 (5pp) doi:10.1088/0022-3727/46/23/235303

Molecular structure-dependent deformations in boron nitride nanostructures subject to an electrical field

Jin Zhang, Chengyuan Wang and Sondipon Adhikari

College of Engineering, Swansea University, Singleton Park, Swansea, Wales SA2 8PP, UK

E-mail: chengyuan.wang@swansea.ac.uk (C Wang)

Received 25 February 2013, in final form 9 April 2013
Published 24 May 2013
Online at stacks.iop.org/JPhysD/46/235303

Abstract

Based on a molecular mechanics approach pre-buckling and buckling deformations are studied for boron nitride nanotubes (BNNTs) and nanosheets (BNNSs) subject to an electrical field. Due to the reverse piezoelectric effect a compressive or shear force is generated for those of zigzag and armchair structures, respectively. As a result, axial deformation and buckling occur for zigzag BNNTs and BNNSs, while a torsional or shear deformation occurs for their armchair counterparts, followed by the corresponding buckling. The critical buckling electrical field is also studied and found to decrease as the aspect ratio of BNNTs and BNNSs increases. Such an effect of the aspect ratio turns out to be more pronounced for the buckling of armchair BNNTs and BNNSs.

(Some figures may appear in colour only in the online journal)

1. Introduction

One dimensional nanomaterials, e.g., carbon nanotubes (CNTs) and boron nitride (BN) nanotubes and two-dimensional nanomaterials, e.g., graphene and BN nanosheets have sparked great interest, due to their novel properties and potential applications in nanodevices. BN nanostructures have a structure analogy of their carbon counterparts (CNTs and graphene), in which alternating boron and nitrogen atoms substitute for carbon atoms.

Similar to carbon nanostructures with exceptional mechanical properties [1–3] BN nanostructures have also been studied intensively and show superior mechanical properties. Golberg *et al* [4] proved that BN nanotubes have a Young's modulus similar to that of CNTs, thus making them as stiffness as CNTs in axial direction. Zheng *et al* [5, 6] tested the effective radial elastic modulus of single-/multi-walled BN nanotubes by atomic force microscopy. The results showed that BN nanotubes exhibit effective radial elastic modulus in the same order of magnitude of CNT modulus. Recently, the torsional stiffness of multi-walled BN nanotubes was observed to be up to one order of magnitude stiffer and stronger than CNTs [7]. For BN nanosheets, the experimental investigation is still limited, the theoretical methods such as the molecular dynamics [8] and molecular mechanics [9] reported their in-plane tensile rigidity varying between 0.26 and 0.28 TPa nm depending on their atomic structures.

In comparison with carbon nanostructures BN nanostructures have several advantages for various applications, for example, they have considerable chemical and thermal stabilities [10], but at the same time they have comparable mechanical properties to carbon nanostructures [4]. Recently, the existence of high axial piezoelectricity has been reported in zigzag BN nanostructures [11–13] which brings new opportunities in developing smart materials. One of these is the energy conversion material by applying large axial electrical fields on the BN nanostructures. However, due to the high piezoelectricity the axial electrical field will generate axial deformations [14] or stresses in the BN nanostructures, which may further trigger the onset of the buckling across the whole BN nanostructures. Thus, an insight investigation of buckling due to an electrical field is essential for the applications of BN nanostructures as energy conversion materials, especially when the field strength is very high.

In this paper the pre-buckling and buckling behaviour of BN nanotubes and nanosheets are investigated by the

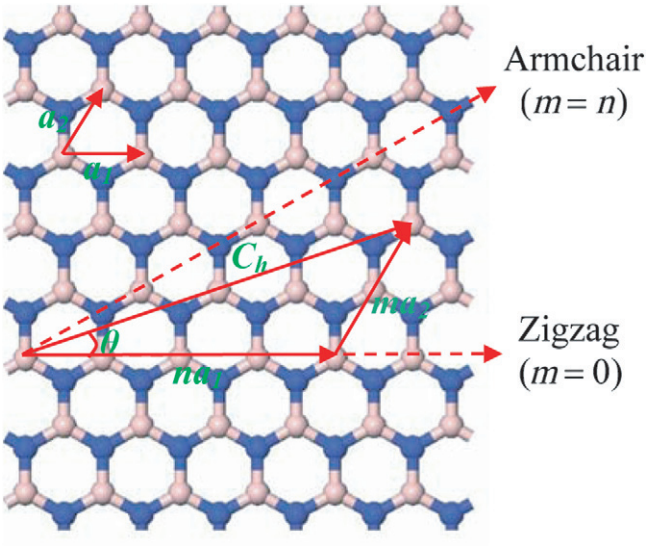

Figure 1. Schematic diagram of a hexagonal BN nanosheet where the pink and the blue balls denote the B and N atoms, respectively.

molecular mechanics approach. The influence of the atomic structures of the BN nanostructures on their deformation and corresponding buckling behaviour is studied. In addition, the effect of the geometry of the nanostructures on the critical buckling axial electrical field is also investigated.

2. Structures of BN nanotubes and nanosheets

The schematic of the BN nanosheets are presented in figure 1 and the BN nanotubes can be considered as BN nanosheet of hexagonal that is rolled up into a hollow seamless cylinder. The atomic structure of BN nanotubes can be described in terms of the tube chirality, which is defined by the chiral vector $\vec{C}_h$ and the chiral angle θ as shown in figure 1. The chiral vector, also known as the roll-up vector, can be described by the following equation:

$$\vec{C}_h = n\vec{a}_1 + m\vec{a}_2. \tag{1}$$

Here the integers n and m are the number of steps along the zigzag bonds of the hexagonal lattice and $\vec{a}_1$ and $\vec{a}_2$ are unit vectors. The chiral angles are 0° and 30° for the two limiting cases which are referred to as zigzag and armchair, respectively. In terms of the chiral vector, a zigzag nanotube is denoted as $(n, 0)$ and an armchair nanotube as (n, n). The chiral vector of the nanotube also defines the nanotube diameter as

$$d = l\sqrt{3(m^2 + mn + n^2)}/\pi \tag{2}$$

where $l = 0.145$ nm is the B–N bond length [15].

3. Molecular structural method for electrical field actuated BN nanostructures

At the atomistic scale, boron and nitride atoms in the hexagonal array of a nanotube and a nanosheet are bonded together by covalent bonds. These covalent bonds have their characteristic bond lengths and bond angles in a three-dimensional space for nanotubes and a two-dimensional space for nanosheets.

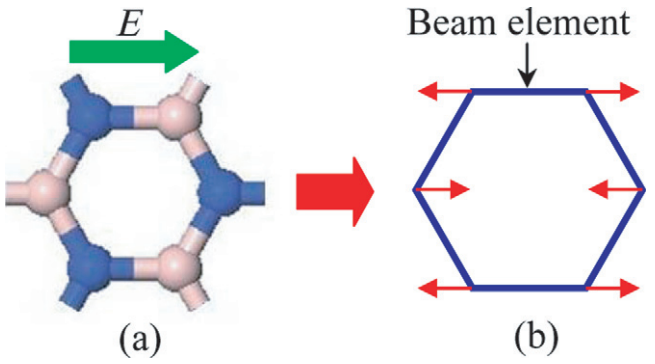

Figure 2. (*a*) A molecular representation of a cell in the BN nanostructure in an electrical field E; (*b*) An equivalent cell for the space frame structure method.

When a nanostructure is subjected to external forces, the displacements of the individual atoms are constrained by these bonds, and the corresponding deformation of the nanostructure is a result of the bond interactions. We assume that the covalent bonds between boron and nitride atoms can be simulated as connecting beam elements with round cross-sections and the atoms as joints of the beam elements with axial stiffness (YA), bending stiffness (YI), and torsional rigidity (GJ) as shown in figure 2. The whole nanostructure is then simulated as a space frame structure. Following the procedure of [16], the direct relationships between the beam stiffness parameters and the force constants can be established as follows:

$$\frac{YA}{l} = k_r, \qquad \frac{YI}{l} = k_\theta, \qquad \frac{GJ}{l} = k_\tau, \tag{3}$$

where Y, G, A, I and J are, respectively, the Young's modulus, shear modulus, cross-sectional area, moment of inertia and polar inertia of the equivalent beam, and l is the bond length (0.145 nm for BN nanostructures). The force constants k_r, k_θ, and k_τ are 4.865×10^{-7} N nm^{-1}, 6.952×10^{-10} N nm rad^{-2}, and 6.255×10^{-10} N nm rad^{-2} for BN nanostructures from the DREIDING force field [17].

The space frame structure method was used widely in the literatures for modelling the mechanical behaviour of carbon and BN nanostructures [9, 16, 18–21]. However, no works on the electrical field induced responses of nanostructures using space frame structure method has been reported. It is widely known that when boron and nitride are combined, the boron atoms each lose three electrons, forming cations (B^{3+}), and the nitride atoms each gain three electrons to form anions (N^{3-}). These ions are then attracted to each other in a 1 : 1 ratio to form BN. When an external electrical field applied in the BN nanostructures as shown in figure 2(*a*) a Coulomb force F_i will be generated on ion i (see figure 2(*b*)) and it can be expressed as

$$F_i = Eq_i, \tag{4}$$

where E is the electric field strength and q_i is the charge on ion i (+3e for B^{3+} and -3e for N^{3-}). This Coulomb model has been used to determine the piezoelectric properties of the gallium nitride nanowires recently [22]. It is found that the piezoelectric property for the bulk gallium nitride obtained from the Coulomb model implemented by using the molecular dynamics simulation was found to agree well with that from the *ab initio* study.

Table 1. Comparison of the calculated tensile rigidity (TPa nm) of the BN structures by the present study and previous literature [8, 23].

	Nanotube		Nanosheet	
	Zigzag	Armchair	Zigzag	Armchair
Present study	0.23–0.26	0.24–0.26	0.26	0.27
Literatures	0.25–0.27 [23]	0.26–0.27 [23]	0.26–0.28 [8]	

4. Results and discussion

In this section the tensile rigidity of the BN nanostructures with different atomic structures, i.e. zigzag and armchair nanotubes and nanosheets, is firstly tested to validate our present method and model. The tensile rigidity of a material is defined as the ratio of the stress to the normal strain in a uniaxial tension test. Here, we follow this definition and simulate the behaviour of BN nanostructures under axial tension. The tensile rigidity of the BN nanostructures from present study is presented in table 1 together with that presented in previous literatures [8, 23] for comparison. It can be seen from table 1 the tensile rigidity depends on the atomic structure of the BN nanostructures and the present results are in a good agreement with those reported in previous studies with relative difference less than 5%.

When an axial electrical field is applied, the mechanical responses of BN nanostructures are shown in figure 3 for a (10, 0) zigzag nanotube (figure 3(*a*)), a (5, 5) armchair nanotube (figure 3(*b*)), a (3, 0) zigzag nanosheet (figure 3(*c*)) and a (3, 3) armchair nanosheet (figure 3(*d*)). In figure 3 the blue lines represent the deformed configurations due to the axial electrical field, while the black lines denote the initial structures. In all simulations the bottom layer atoms of the nanostructures are fixed while the top layer atoms are free. We can see from figure 3 that although there is no mechanical force applied, the BN nanostructures deformed due to the resultant of the Coulomb forces on all ions. Moreover, it also can be seen from figure 3 that the deformation of BN nanostructures induced by the electrical field strongly depends on their molecular structures. When an axial electrical field is applied, an axial deformation occurs in the zigzag nanotubes and nanosheets (see figures 3(*a*) and (*c*)) and a shearing deformation occurs in armchair nanotubes and nanosheets (see figures 3(*b*) and (*d*)).

The different behaviours between zigzag and armchair BN nanostructures in the electric field arise from their distinctly different structures. In zigzag nanostructures, the B and N atoms distribute along the tube or sheet axis layer by layer, giving rise to axial but no shearing (or torsional) spontaneous polarization [13] and further only giving an axial piezoelectric constant e_{11} [13]. In contrast, in armchair BN nanostructures, each layer has the same number of B or N atoms, which gives a shearing (or torsional) spontaneous polarization but no axial spontaneous polarization exists and thus only gives a shearing piezoelectric constant e_{14} for nanosheets or a torsional piezoelectric constant e_{14} for nanotubes [13]. From the continuum mechanics viewpoint, when an axial external electrical field E is applied, the stress in the BN nanostructure due to the electrical field can be expressed as $\sigma_{1j} = Ee_{1j}$ ($j = 1$ for zigzag structure and $j = 4$ for armchair structure). This illustrates that a compression exists in zigzag nanostructures and a shearing (or torsion) exists in armchair nanostructures when an axial electrical field applied.

Form the above discussion it is known that an axial electrical field will generate an equivalent compression in the zigzag BN nanostructures (both of nanotubes and nanosheets), an equivalent torsion in the armchair nanotubes and an equivalent shearing in the armchair nanosheets. As we illustrated above, all of these forces are measured by the strength of the electrical field. When the strength of the applied axial electrical field increases beyond a critical value E_{cr} the BN structures will lose their stability. Subsequently, we shall give an insight discussion on the buckling of the BN nanostructures induced by the applied axial electrical field. The buckling analysis was performed by initially applying a reference level of axial electrical field to the BN nanostructures (usually taken as $1\,\mathrm{V\,nm^{-1}}$). Then a standard linear static analysis was carried out for the BN structure to obtain its geometric stiffness matrix. With the stiffness matrix the critical buckling electrical field of the BN structure can be calculated by solving an eigenvalue problem. The readers can refer to [19] for more details. The calculated critical buckling axial electrical field E_{cr} of the clamped-free (21, 0) zigzag ($d = 1.68\,\mathrm{nm}$) and (12, 12) armchair ($d = 1.66\,\mathrm{nm}$) BN nanotubes is plotted as a function of the nanotube aspect ratio L/d in figure 4 where L is the nanotube length. We can see from figure 4 that E_{cr} decreases as the ratio L/d increases both for zigzag and armchair nanotubes. However, compared with the zigzag nanotubes the electrical field induced buckling of the armchair nanotube is more sensitive to the change of the geometric size of the nanotube, e.g., for armchair nanotubes E_{cr} decreases by 45% as the ratio L/d increases form 2.15 to 5.46, while for zigzag nanotubes E_{cr} decreases by only 12% as the ratio L/dincreases from 2.11 to 5.34. Moreover, from figure 4 we can also observe that when an axial electrical field is applied, the armchair nanotube is more stable than the zigzag nanotube. This is because E_{cr} of armchair nanotube is much larger than that of the zigzag nanotube, e.g., E_{cr} of armchair nanotube with $L/d = 2.58$ is about $19\,\mathrm{V\,nm^{-1}}$ which is about 4 times of that of the zigzag nanotube with $L/d = 2.50$. The buckling modes of the zigzag nanotube with $L/d = 5.46$ and the armchair nanotube with $L/d = 5.34$ are also presented as insets of figure 4. It is seen from the figure that under the applied electrical field, the zigzag nanotube buckles in the same way when it is subjected to an axial mechanical force, while the buckling mode of the armchair nanotube is identical to the one when it is under a torsion [24, 25].

Finally, the electrical field induced buckling of rectangular BN nanosheets was studied and shown graphically in figure 5 for (17, 0) zigzag and (10, 10) armchair nanosheets. Here, a pair of parallel sides are free (i.e., the length a) while the other two sides represented by the black bands in figure 5 are clamped (i.e., the width b). An external electric field is applied along the direction of the length. In this work particular attention was placed on the effect of the aspect ratio a/b on the critical buckling axial electrical field (E_{cr}). As shown in figure 5, E_{cr} decreases with the increasing ratio a/b as far as zigzag or

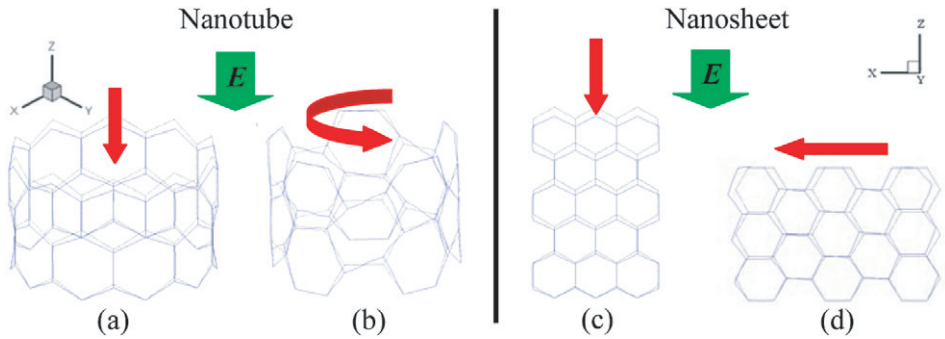

Figure 3. The axial electrical field induced deformation in (*a*) zigzag BN nanotubes, (*b*) armchair BN nanotubes, (*c*) zigzag BN nanosheets and (*d*) armchair BN nanosheets. Here the blue lines present the deformed configurations due to the axial electrical field E and the black lines denote the initial structures. The red arrows here represent the direction of the equivalent stresses induced by the same electric field E in BN nanotubes and nanosheets of different molecular structures.

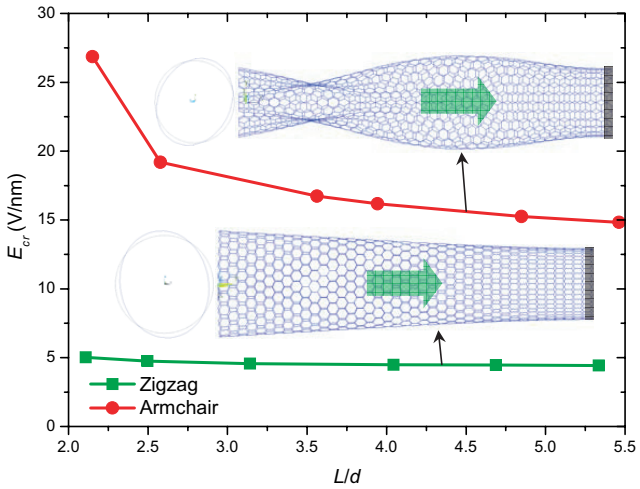

Figure 4. The aspect ratio-dependence of the critical buckling electrical field obtained for (21, 0) zigzag and (12, 12) armchair BN nanotubes. The insets show the buckling modes of the BN nanotubes. Here the black bands show the clamped edges and the green arrows indicate the direction of the applied electrical field.

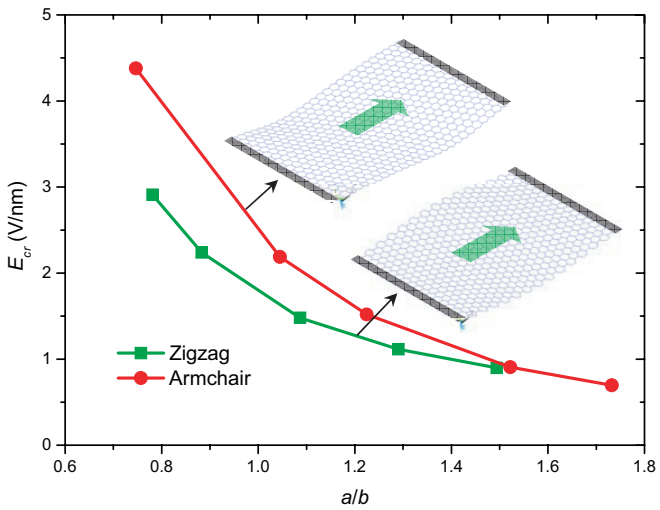

Figure 5. The aspect ratio-dependence of the critical buckling electrical field obtained for (17, 0) zigzag and (10, 10) armchair BN nanosheets. The insets show the buckling modes of the BN nanosheets. Here the black bands show the clamped edges and the green arrows indicate the direction of the applied electrical field.

armchair nanosheets are concerned. Specifically, E_{cr} of the zigzag nanosheets is more sensitive to the variation of a/b than that of the armchair ones. This behaviour is found to be similar to that of the nanotubes observed above. Further, the insets of figure 5 show the buckling modes of the zigzag and the armchair nanosheets with the aspect ratio a/b around 1.5. It is seen from the figure that under the applied electrical field, the zigzag nanosheet buckles in the same way when it is subjected to an axial mechanical force, while the buckling mode of the armchair nanosheet is identical to the one when it is under a shearing force [26].

5. Conclusions

The pre-buckling and buckling behaviours of boron nitride nanotubes and nanosheets induced by an applied axial electrical field are investigated based on a molecular mechanics approach. The novelty of the paper is in understanding and highlighting the intricate interplay between the electrical field and the mechanical deformations. The results show that the deformation of nanostructures induced by the electrical field depends on their molecular structures, i.e., an axial deformation occurs in zigzag nanostructures and a shearing deformation occurs in armchair nanostructures. In particular, when the axial electrical field increases beyond a critical value noted as E_{cr} an axial buckling occurs in zigzag nanotubes and nanosheets, a torsion buckling occurs in armchair nanotubes and a shearing buckling occurs in armchair nanosheets. It is found that E_{cr} decreases as the aspect ratio increases in both zigzag and armchair nanostructures, however, compared with the zigzag nanostructures E_{cr} is more sensitive to the change of the aspect ratio of the armchair nanostructures. The different responses between different molecular structures are found to be a result of the distinct direction of polarizations in the corresponding nanostructures.

Acknowledgments

JZ acknowledges the support from the China Scholarship Council (CSC). SA acknowledges the support from the Royal Society through the award of Wolfson Research Merit Award.

References

[1] Treacy M M J, Ebbesen T W and Gibson J M 1996 *Nature* **381** 678
[2] Hernandez E, Goze C, Bernier P and Rubio A 1998 *Phys. Rev. Lett.* **80** 4502
[3] Sanchez-Portal D, Artacho E, Soler J M, Rubio A and Ordejon P 1999 *Phys. Rev.* B **59** 12678
[4] Golberg D, Bando Y, Huang Y, Terao T, Mitome M, Tang C and Zhi C 2010 *ACS Nano* **4** 2979
[5] Zheng M, Ke C H, Bae I T, Park C, Smith M W and Jordan K 2012 *Nanotechnology* **23** 095703
[6] Zheng M, Chen X M, Bae I T, Ke C H, Park C, Smith M W and Jordan K 2012 *Small* **8** 116
[7] Garel J, Leven I, Zhi C Y, Nagapriya K S, Popovitz-Biro R, Golberg D, Bando Y, Hod O and Joselevich E 2012 *Nano Lett.* **12** 6347
[8] Mortazavi B and Remond Y 2012 *Physica* E **44** 1846
[9] Boldrin L, Scarpa F, Chowdhury R and Adhikari S 2011 *Nanotechnology* **22** 505702
[10] Chen Y, Zou J, Campbell S J and Caer G L 2004 *Appl. Phys. Lett.* **84** 2430
[11] Mele E J and Kral P 2002 *Phys. Rev. Lett.* **88** 056803
[12] Nakhmanson S M, Calzolari A, Meunier V, Bernholc J and Nardelli M B 2003 *Phys. Rev.* B **67** 235406
[13] Sai N and Mele E J 2003 *Phys. Rev.* B **68** 241405
[14] Dai Y T, Guo W L, Zhang Z H, Zhou B and Tang C 2009 *J. Phys. D: Appl. Phys.* **42** 085403
[15] Pokropivnyi V V 2001 *Powder Metall. Met. Ceram.* **40** 582
[16] Li C Y and Chou T W 2003 *Phys. Rev.* B **68** 073405
[17] Mayo S L, Olafson B D and Goddard W A 1990 *J. Phys. Chem.* **94** 8897
[18] Li C Y and Chou T W 2004 *Appl. Phys. Lett.* **84** 121
[19] Li C Y and Chou T W 2004 *Mech. Mater.* **36** 1047
[20] Li C Y and Chou T W 2006 *J. Nanosci. Nanotechnol.* **6** 54
[21] Jafari A, Khatibi A A and Mashhadi M M 2012 *J. Comput. Theor. Nanosci.* **9** 461
[22] Zhang J, Wang C Y, Chowdhury R and Adhikari S 2013 *Scripta Mater.* **68** 627
[23] Kudin K N, Scuseria G E and Yakobson B I 2001 *Phys. Rev.* B **64** 235406
[24] Ansari R and Rouhi S 2011 *Physica* E **43** 58
[25] Li Y F, Yu H Q, Li H, Zhang K, An C G, Liew K M and Liu X F 2010 *J. Phys. Chem.* C **114** 11421
[26] Duan W H, Gong K and Wang Q 2011 *Carbon* **49** 3107